

Bound state and hydrodynamic interaction of microrods in chiral nematic liquid crystals

Muhammed Rasi M¹, Ravi Kumar Pujala², Sathyanarayana Paladugu², and Surajit Dhara^{1*}

¹*School of Physics, University of Hyderabad, Hyderabad-500046, India*

²*Department of Physics, Indian Institute of Science Education and Research, Tirupati, Andhra Pradesh 517507, India*

(Dated: December 23, 2024)

In a striking departure from the pair interaction of spherical microparticles in chiral nematic liquid crystals we show that a pair of microrods are self-trapped in effective elastic potentials which are separated by a fixed distance forming a bound state. The robustness of the bound state is demonstrated by applying external electrical and mechanical forces that perturbs their equilibrium position as well as orientation. In the bound state the microrods interact through the hydrodynamic forces which are determined from the measurements of the correlated thermal fluctuations in their position using two-particle cross-correlation spectroscopy. These findings reveal unexplored aspects of liquid-crystal dispersions which are important for understanding their collective behaviour and dynamics.

Microparticles in nematic liquid crystals (NLCs) create spatial deformation of the director \hat{n} (mean molecular orientation), and induce topological point or line defects [1–3]. The defect structures and the ensuing elastic distortion mediated long-range interactions have created immense interests in recent years owing to the potential application for designing two and three dimensional colloidal crystals [4, 5]. When the dispersing medium is a chiral nematic the director twists in space, exhibiting a number of interesting defects that includes vortex-like nonsingular defects [6, 8], knots and links [9], torons [10], skyrmions [11, 12] etc. These defects and the resulting elastic interaction of spherical microparticles often leads to metastable [13] and reconfigurable states [9, 14, 15].

Apart from the elastic interaction, theoretically it has been shown that the hydrodynamic interaction of microparticles in liquid crystals plays an important role in their dynamics and assembly [16–18]. But the effect of the latter is not directly explored experimentally. The hydrodynamic interaction has been studied directly in aqueous colloidal systems by optically trapping two Brownian particles using laser tweezers [19, 20]. However, the particles in LCs can not be directly trapped by laser tweezers in the conventional way [21, 22] thus making the direct measurement of hydrodynamic interaction problematic in LCs.

In this letter we study individual silica microrods in chiral NLCs and show that the elastic pair interaction leads to a bound state, in which they are self-trapped in elastic potentials, separated by a fixed distance. We show that the trapping is robust against external perturbations that tends to change their position as well as orientation. Our experiments present a direct measurement of the hydrodynamic interaction of microparticles revealing an unexplored aspect of liquid crystal dispersions.

Silica microrods are synthesised by a wet chemical method following a procedure described by Kuijk *et*

al. [23, 24]. The average length and diameter are 6 μm and 800 nm, respectively and one end of the microrods is round-shaped as shown in Fig.1(a). The microrods were coated with octadecyldimethyl-3-trimethoxysilyl propyl-ammonium chloride (DMOAP) before dispersing into the chiral NLCs for obtaining perpendicular or homeotropic orientation of the director \hat{n} . The chiral NLCs were prepared by doping a chiral agent 4-cyano-40-(2-methylbutyl)-biphenylene (CB15) in 4-n-pentyl-4-cyanobiphenyl (5CB) nematic liquid crystal. The concentration of CB15 was adjusted to vary the helical pitch, which was measured using a wedge cell [25]. The dispersions were studied in planar cells, which are prepared by two parallel glass plates (15 mm \times 10 mm) coated with the polyimide AL-1254 (Nissan Chemicals). The plates were rubbed in an antiparallel way before assembling so that the helix axis of the chiral NLC is perpendicular to the plane of the substrate as shown in Fig.1(b). The pitch was adjusted in a cell of gap d such that the nematic structure is twisted by multiples of half-pitch i.e., $d = N(p/2)$ which is denoted here as $N\pi$ cell (Fig.1(b)). An infrared laser tweezers setup (Aresis, Tweez 250Si) attached to an inverted optical polarising microscope (Nikon Eclipse Ti-U) was used in the experiments [26–28]. The laser trap movement was controlled by an acousto-optic deflector (AOD) and computer. The motion of the microrods were video recorded using a 60X water immersion objective (Nikon NIR Apo) and a camera at the rate of 50 frames per second. The centre of the microrod was measured from the video-microscopy with a resolution of ± 20 nm [29, 30]. The autocorrelation and cross-correlation functions of the position fluctuations were computed using the Mathematica program.

We work in the dilute concentration regime where most of the microrods are dispersed singly throughout the cell. At first, we study the LC-microrod dispersions in a 2π cell and observe that the majority of the microrods are oriented perpendicular to the rubbing direction (Fig.1(c)). Although the surrounding elastic distortion of the microrod is clearly visible, the structure of the defect is unclear unlike the case of a microsphere (Fig.1(d)). We

* sdsp@uohyd.ernet.in

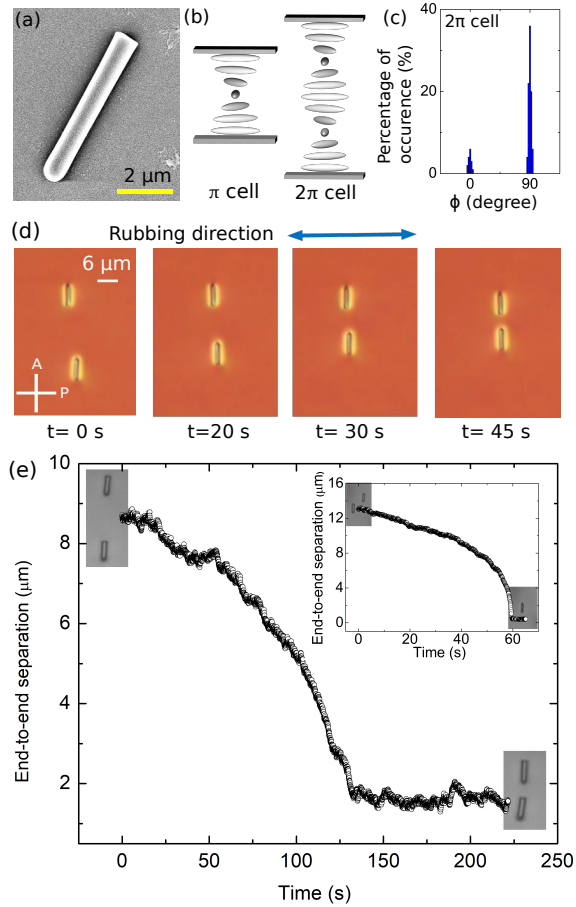


FIG. 1. (a) Field emission scanning electron microscope (FESEM) image of a silica microrod. (b) Director twist in π and 2π cell. (c) Percentage of microrods oriented parallel ($\phi \simeq 0^\circ$) and perpendicular ($\phi \simeq 90^\circ$) with respect to the rubbing direction in 2π cell. (d) Snapshots of interacting microrods at different times taken using polarising optical microscope. Horizontal arrow indicates the rubbing direction. P, A indicates polariser and analyser. (e) End-to-end separation of two interacting microrods in 2π cell (Movie S1). The inset shows the end-to-end separation in a planar, homogeneous nematic (5CB).

study the pair interaction of microrods orientated perpendicular to the rubbing direction in a 2π cell. Two coaxial microrods were positioned at a certain distance away with the help of the laser tweezers and allowed them to interact freely by switching off the laser. Figure 1(d) shows a few snapshots at different times while they are approaching to each other. With increasing time the end-to-end separation decreases and eventually the microrods are self-confined or trapped at a fixed separation forming a bound state as shown in Fig.1(e). The mean separation between the microrods in the bound state (beyond 130 s) is $1.65 \mu\text{m}$ and it remains fixed forever (see Fig.S1). It appears as if the microrods are trapped in the global energy minimum. Similar behaviour is also observed in cells with different chiralities except the end-to-end separation

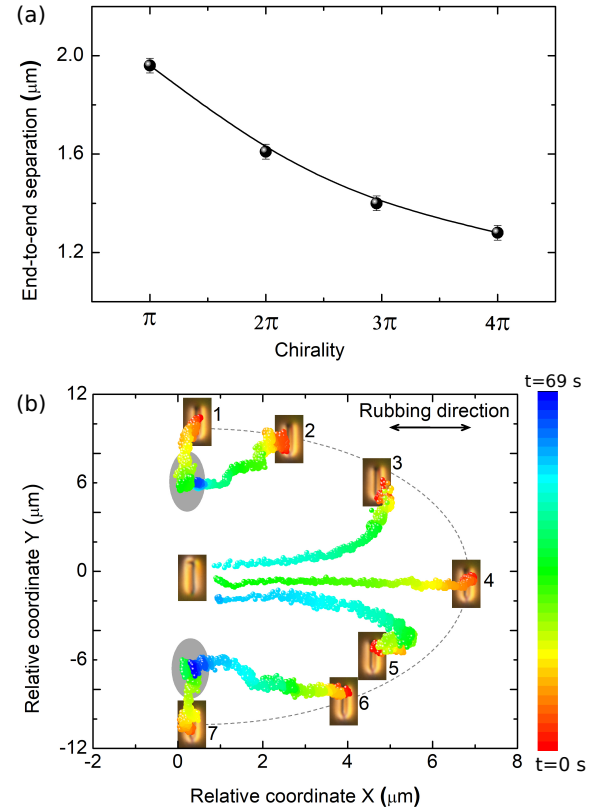


FIG. 2. (a) Variation of end-to-end separation with chirality in the bound state. (b) Time coded trajectories (relative coordinates) of microrods approaching from different starting positions in 2π cell. By “relative coordinate” we mean relative to the starting point of each trajectory. Shaded regions indicate where the approaching particle is permanently bound with the central particle.

decreases moderately with increasing chirality as shown in Fig.2(a). The interaction in chiral NLCs is noticeably different than that is observed in a planar or homogeneous nematic where the end-to-end separation is reduced to zero as shown in the inset of Fig.1(e). Spherical microparticles in chiral NLCs exhibit metastable states due to the screening of chiral interaction in which the microspheres are temporarily held at a fixed separation for a certain period of time and eventually they are attracted and joined together [13]. The striking result of our experiment is that the microrods are permanently self-trapped forming a stable bound state without merging. The bound state is result of complete screening of the far and the near field elastic pair interaction. The anisotropy of the pair interaction was studied by looking at the relative time coded trajectories of microrods released from different starting positions with respect to a central microrod as shown in Fig.2(b). Microrods starting from the positions 1,2,6 and 7 are attracted to form the bound state whereas the microrods released from the starting positions 3,4,5, are merge eventually.

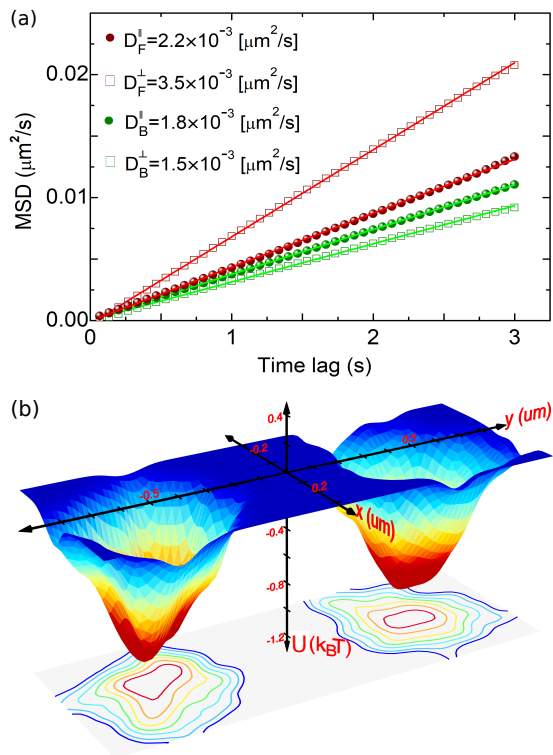


FIG. 3. (a) Mean squared displacements (MSDs) of a free microrod (red symbols) and a bound microrod (green symbols) in 2π cell. The subscripts F and B stands for free and bound microrods, respectively and the superscripts \parallel and \perp indicate motions parallel and perpendicular to the rubbing direction. (c) Confining potentials of the bound microrods. Separation along the y -direction is normalised.

In the bound state the Brownian motions due to thermal agitations of the microrods are clearly observed (see Movie S1). The self-diffusion coefficients $D_B^{\parallel,\perp}$ of a bound microrod and $D_F^{\parallel,\perp}$ of a free or isolated microrod (where \parallel and \perp refers in relation to the rubbing direction) were obtained from the mean squared displacement. Figure 3(b) shows that $D_B^{\perp} \simeq 0.4D_F^{\perp}$ and $D_B^{\parallel} \simeq 0.8D_F^{\parallel}$ i.e., the diffusion coefficients in the bound state are reduced considerably than that of a free microrod as expected. We measured the effective confining potentials from the study of the Brownian statistics of the microrods in the region accessible by thermal agitations [31]. In equilibrium the probability density of the particle position is given by $p(x) = C \exp[-U(x)/k_B T]$, where C is the normalisation constant and $U(x)$ is the confining potential. The potential is obtained from the normalised histogram of the confined particle's positions and given by $U(x) = -\ln[p(x)]$. Figure 3(b) shows the confining potentials of the microrods at a normalised centre-to-centre distance. The depth of the potential energy is $\sim k_B T$ and highly asymmetric as expected (see contour plots). Assuming the potentials are harmonic, the effective stiffness constants k_x (along rubbing direction) and k_y (perpendicular to the

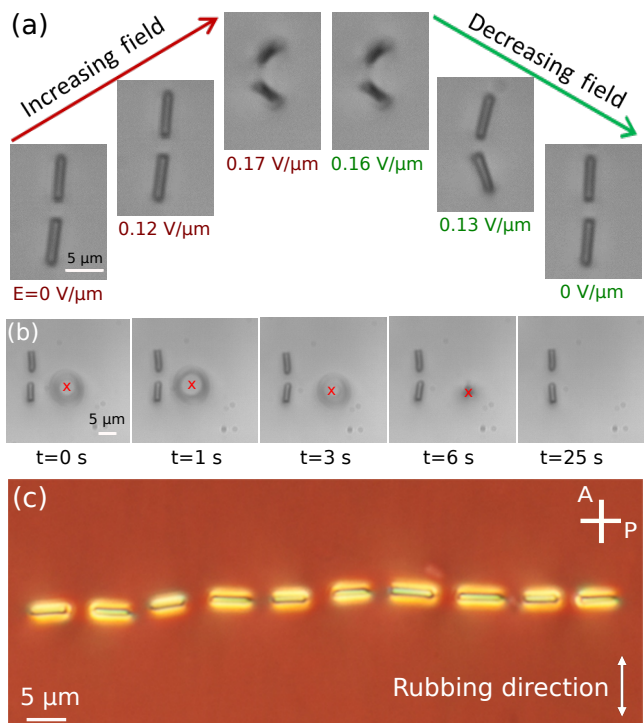


FIG. 4. (a) Effect of AC electric field ($f = 1$ kHz) on the bound state in 2π cell (Movie S2) (b) Effect of mechanical force applied by the laser tweezers on the bound state. (Movie S3) (c) A linear chain of 10 microrods forming successive bound states (Movie S4). They were guided to assemble with the help of a dynamic laser tweezers setup.

rubbing direction) are given by $k_x = 4.3 \pm 0.1 \times 10^{-6}$ N/m and $k_y = 4.8 \pm 0.1 \times 10^{-6}$ N/m. The stiffness constants of the confining potentials are comparable to that of the low power optical traps [19, 33].

To test the robustness of the bound state we applied an external AC electric field that perturbs the position and orientation of the microrods (Movie S2). Fig.4(a) shows some snapshots at different field strengths. The maximum field was restricted to the Freedericksz threshold value ($\simeq 0.2$ V/ μm) so that the far field director remains unaffected. Beyond $\simeq 0.12$ V/ μm , the microrods are displaced (see Fig.S2) and they also tilt simultaneously in the plane as well as out of the plane. The initial state is recovered when the electric field is switched off. We further checked the stability by applying a mild mechanical force with the help of the laser tweezers as shown in Fig.4(b). It is observed that the bound state is stable against the elastic distortion created by the trap surrounding the microrods (Movie S3). With the help of the laser tweezers we have created an assembly of several microrods in the form of a linear chain as shown in Fig.4(c). Here the microrods are virtually linked through the successive bound states. The chain is little zigzag which could be due to the slight variation in the length and diameter of the microrods. Nevertheless the chain is stable against thermal fluctuations and mild perturb-

ing force applied by the laser tweezers (Movie S5) and remains unchanged even after a few days (Movie S4). It may be mentioned that although one end of the microrods is round-shaped the bound state formation does not depend on the shape of the facing ends.

In what follows we study the hydrodynamic interaction of the microrods in the bound state. Hydrodynamic interaction of particles in aqueous solution has been studied by optically trapping a pair of microspheres at varying proximity [19, 20]. In our experiment the bound state of the microrods is a reminiscent of similar experimental situation, providing an opportunity to measure directly the hydrodynamic interaction. We measure the position and calculate the autocorrelation and cross-correlation functions. In the framework of Langevin dynamics for a low Reynolds number system the autocorrelation and the cross-correlation functions of position vectors of the two particles along y -direction (perpendicular to the rubbing direction) are given by [19]

$$\begin{aligned} \langle R_1(t)R_1(0) \rangle &= \langle R_2(t)R_2(0) \rangle \\ &= \frac{k_B T}{2k_y} (e^{-t(1+\epsilon)/\tau} + e^{-t(1-\epsilon)/\tau}) \end{aligned} \quad (1)$$

$$\begin{aligned} \langle R_1(t)R_2(0) \rangle &= \langle R_2(t)R_1(0) \rangle \\ &= \frac{k_B T}{2k_y} (e^{-t(1+\epsilon)/\tau} - e^{-t(1-\epsilon)/\tau}) \end{aligned} \quad (2)$$

where τ is the relaxation time and ϵ is a dimensionless parameter. The autocorrelation and cross-correlation functions measured in π and 2π cells and the theoretical fits to Eq.(1) and Eq.(2) are shown in Fig.5(a). The parameters obtained from the fittings are given by $\tau = 0.64 \pm 0.01$ s and $\epsilon = 0.10 \pm 0.01$. The autocorrelation function decay exponentially as expected whereas a strong time delayed-anticorrelation is observed with a pronounced minimum at $t_{min} \approx \tau \simeq 0.64$ s. It means the hydrodynamic interaction is asymmetric as one microrod moves it tends to drag the other and the correlated fluctuations relax faster than the anticorrelated fluctuations. We directly measure ϵ from the particle separation and τ from the effective confining potentials. τ is given by the ratio of the friction coefficient ζ_y and the stiffness constant k_y of the potential i.e., $\tau = \zeta_y/k_y$. The parameter ϵ describes the ratio of the mobility of the particle and the strength of the hydrodynamic coupling and expressed as $\epsilon \approx 3a/2r$, where r is the mean separation and a is the radius of the particle [19]. From the measured diffusion coefficient (Fig.3(a)) we obtain $\zeta_y = 2.8 \times 10^{-6}$ Kg/s using Stokes-Einstein relation and $k_y = 4.8 \times 10^{-6}$ N/m from the confining potentials (Fig.3(b)). Taking radius of the microrod $a = 0.4 \mu\text{m}$ and centre-to-centre separation $r \simeq 7 \mu\text{m}$ the measured parameters are $\tau = 0.58$ s and $\epsilon \simeq 0.09$. These parameters are in good agreement with those obtained from the fitting of the autocorrelation and cross-correlation functions. It is also observed

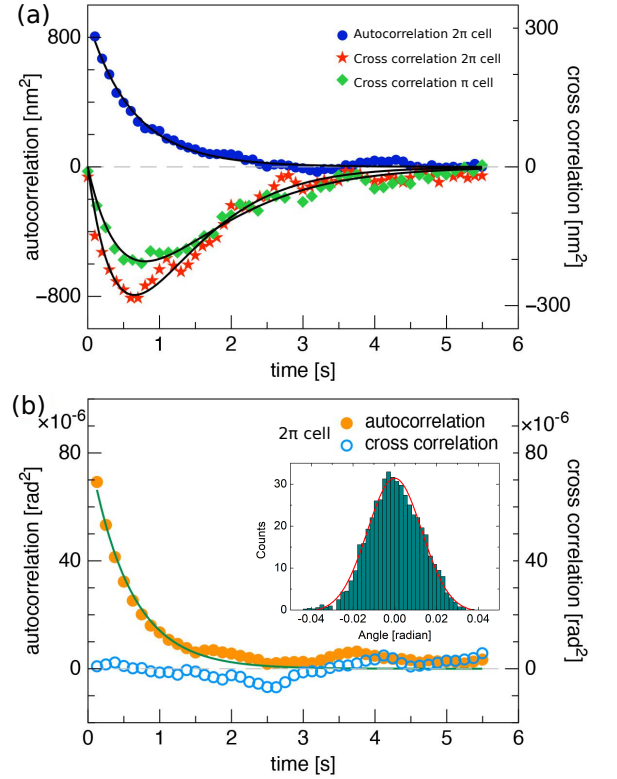


FIG. 5. (a) Longitudinal autocorrelation $\langle R_1(t)R_1(0) \rangle$ (blue circles) and cross-correlation $\langle R_1(t)R_2(0) \rangle$ (green diamonds and red stars) functions of the two microrods in π and 2π cells. Solid lines represent the best fit to Eq.(1). (b) Autocorrelation function $\langle \theta_1(t)\theta_1(0) \rangle$ (solid circles) and cross-correlation function $\langle \theta_1(t)\theta_2(0) \rangle$ of orientational fluctuations (open circles) of two microrods in 2π cell. θ_1 and θ_2 are measured with respect to the vertical axis (see Fig.1(d)). Only every third of the experimental data points is shown. The inset shows the histogram of a orientational deviation.

from Fig.5(a) that the depth of the minima in 2π cell is higher than that of π cell. In 2π cell the particles are closer than π cell (Fig.2(a)) hence, the result is consistent with the prediction that the strength of the hydrodynamic coupling is inversely proportional to the separation [19].

In the bound state the orientational fluctuations of the microrods are observed clearly. The orientational fluctuations θ_1 and θ_2 of the long axis of the microrods is measured with respect to a vertical axis (see Fig.1(d)). The histogram of the orientational fluctuations is a Gaussian as shown in the inset of Fig.5(b). We measure the autocorrelation $\langle \theta_1(t)\theta_1(0) \rangle$ and cross-correlation $\langle \theta_1(t)\theta_2(0) \rangle$ functions of the orientational fluctuations. Figure 5(b) shows that the autocorrelation function decays exponentially and it can be fitted well to $\sim e^{-t/\tau_o}$ with a decay constant $\tau_o = 56$ ms. This value is comparable to the effective director relaxation time of 5CB liquid crystal ($\simeq 50$ ms) measured by the dynamic

Freedericksz transition [32]. The crosscorrelation function is almost zero, suggesting that the orientational fluctuations are not coupled hydrodynamically.

Three further comments are in order. First, the relaxation time τ of the autocorrelation function of position in the chiral NLCs is 0.64 s which is 15 times larger than that of a microsphere in water (43 ms) [19]. This is expected due to the larger flow viscosity of the liquid crystal ($\eta_{||}^{5CB} \simeq 20$ mPas) [36] with respect to that of the water ($\eta_W \simeq 1$ mPas). Secondly, the effect of electrostatic repulsion in the present experiments is absent as the microrods are uncharged. Thirdly, although the theoretical technique adapted here is described for hydrodynamic interactions in low Reynolds number fluid systems we expect this to be valid as the Reynolds number (R_e) of NLCs is much smaller than 1 ($R_e \sim 10^{-4} - 10^{-5}$) [34, 35].

In conclusion, two collinear silica microrods aligned perpendicular to the rubbing direction in chiral nematic liquid crystals are self-trapped in their mutual elastic potentials which are separated by a fixed distance forming

a stable bound state. The bound state is highly stable and robust against the influence of external electrical and mechanical perturbations applied by an AC electric field and the laser tweezers. In the bound state the positional fluctuations of the microrods are hydrodynamically coupled whereas their orientational fluctuations are uncoupled. The correlation relaxation time of hydrodynamic interaction in chiral nematic liquid crystals is more than one order of magnitude larger than that in aqueous suspensions. Apart from the passive nematics, the hydrodynamic interaction in active nematic dispersions could be important for understanding the collective behaviour and dynamic structures in concentrated suspensions.

SD acknowledges the support from the Department of Science and Technology, Govt. of India (DST/SJF/PSA-02/2014-2015), and DST-PURSE-II. Ravi Kumar Pujala acknowledges DST for INSPIRE Faculty Award Grant [DST/INSPIRE/04/2016/002370] and Core Research Grant [CRG/2020/006281] from SERB. P.S. acknowledges IISER Tirupati for the research funding. M.R.M acknowledges CSIR fellowship.

-
- [1] I. Muševič, *Liquid Crystal Colloids*, Springer Cham, Switzerland (2017).
- [2] I. I. Smalyukh, *Annual Review of Condensed Matter Physics, Liquid Crystal Colloids*, Annu. Rev. Condens. Matter Phys. **9**, 207 (2018).
- [3] H. Stark, Phys. Rep. **351**, 387 (2001).
- [4] I. Muševič, M. Škarabot, U. Tkalec, M. Ravnik and S. Žumer, Science **313**, 954 (2006).
- [5] A. Nych, U. Ognysta, M. Skarabot, M. Ravnik, S. Zumer and I. Musevic, Nat. Commun., **4**, 1489 (2013).
- [6] P. Poulin, V. Cabuil and D. A. Weitz, Phys. Rev. Lett. **79**, 4862 (1997).
- [7] U. Tkalec, M. Ravnik, S. Žumer and I. Muševič, Phys. Rev. Lett. **103**, 127801 (2009).
- [8] U. Tkalec, M. Ravnik, S. Žumer and I. Muševič, Phys. Rev. Lett. **103**, 127801 (2009).
- [9] U. Tkalec, M. Ravnik, S. Čopar, S. Žumer and I. Muševič, Science **333**, 62 (2011).
- [10] J. S. Evans, P. J. Ackerman, D. J. Broer, J. vandeLage-maat and I. I. Smalyukh, Phys. Rev. E **87**, 032503 (2013).
- [11] P. J. Ackerman, T. Boyle and I. I. Smalyukh, Nat. Commun. **8**, 673 (2017).
- [12] G. Posnjak, S. Čopar and I. Muševič, Sci. Rep. **6**, 26361 (2016).
- [13] V. S. R. Jampani, M. Škarabot, S. Čopar, S. Žumer and I. Muševič, Phys. Rev. Lett. **110**, 177801 (2013).
- [14] V. S. R. Jampani, M. Skarabot, M. Ravnik, S. Čopar, S. Žumer, I. Muševič, Phys. Rev. E **84**, 031703 (2011).
- [15] M. Ravnik, M. Skarabot, S. Žumer, U. Tkalec, I. Poberaj, D. Babic, N. Osterman and I. Muševič, Phys. Rev. Lett. **99**, 247801 (2007).
- [16] K. Stratford, A. Gray, J. S. Lintuvuori, J. Stat. Phys. **161**, 1496 (2015).
- [17] G. Foffano, J.S. Lintuvuori, A. Tiribocchi and D. Marenduzzo, Liq. Cryst. Rev. **2**(1), 1 (2014).
- [18] J. S. Lintuvuori, K. Stratford, M. E. Cates, and D. Marenduzzo, Phys. Rev. Lett. **105**, 178302 (2010).
- [19] J-C Meiners and S. R. Quake, Phys. Rev. Lett. **82**, 2211 (1999).
- [20] P. Bartlett, S. I. Hendersons and S. J. Mitchell, Phil. Trans. R. Soc. Lond. A **359**, 883 (2001).
- [21] M. Skarabot *et al.*, Phys. Rev. E **73**, 021705 (2006).
- [22] I. Muševič, M. Škarabot, D. Babič, N. Osterman, I. Poberaj, V. Nazarenko, and A. Nych, Phys. Rev. Lett. **93**, 187801 (2004).
- [23] A. Kuijk, A. V. Blaaderen and A. Imhof, J. Am. Chem. Soc. **133**, 2346 (2011).
- [24] M. Rasi, R. K. Pujala and S. Dhara, Scientific reports **9**, 4652 (2019).
- [25] I. Podolsky, O. Banji and P. Rudquist, Liq. Cryst. **35**, 789 (2008).
- [26] K. P. Zuhail and S. Dhara, Appl. Phys. Lett. **106**, 211901 (2015).
- [27] K. P. Zuhail and S. Dhara, Soft Matter **12**, 6812 (2016).
- [28] M. Rasi M, K. P. Zuhail, A. Roy and S. Dhara, Phys. Rev. E **97**, 032702 (2018).
- [29] K. P. Zuhail, P. Sathyanarayana, D. Seč, S. Čopar, M. Škarabot, I. Muševič and S. Dhara, Phys. Rev. E **91**, 030501(R) (2015).
- [30] M. V. Rasna, L. Cmok, D. R. Evans, A. Mertelj and S. Dhara, Liq. Cryst. **42**, 1059 (2015).
- [31] N. Osterman, Computer Physics Communications **181**, 1911 (2010).
- [32] We measured director relaxation time $\tau_o \simeq 50$ ms using dynamic Freedericksz transition in a planar cell of 5CB at room temperature in a cell of thickness 5 μm .
- [33] F. Belloni, S. Monneret, F. Monduc, and M. Scordia, Opt. Express **16**, 9011(12) (2008).
- [34] O. D. Lavrentovich, Curr. Opin. Colloid Interface Sci. **21**, 97 (2016).
- [35] D. K. Sahu, S. Kole, S. Ramaswamy and Surajit Dhara, Phys. Rev. Res. **2**, 032009(R) (2020).

- [36] A. G. Chimielewski, *Mol. Cryst. Liq. Cryst.* **132**, 339 (1986).